Simultaneous optimal damper placement using oil, hysteretic and inertial mass dampers

Yu Murakami, Katsuya Noshi, Kohei Fujita, Masaaki Tsuji and Izuru Takewaki[*]

*Department of Architecture and Architectural Engineering, Kyoto University
Kyotodaigaku-Katsura, Nishikyo-ku, Kyoto 615-8540, Japan*

Abstract. Oil, hysteretic and inertial mass dampers are representatives of passive dampers used for smart enhancement of seismic performance of building structures. Since oil dampers have a nonlinear relief mechanism and hysteretic dampers possess nonlinear restoring-force characteristics, several difficulties arise in the evaluation of buildings including such dampers. The purpose of this paper is to propose a practical method for simultaneous optimal use of such dampers. The optimum design problem is formulated so as to minimize the maximum interstory drift under design earthquakes in terms of a set of damper quantities subject to an equality constraint on the total cost of dampers. The proposed method to solve the optimum design problem is a successive procedure which consists of two steps. The first step is a sensitivity analysis by using nonlinear time-history response analyses, and the second step is a modification of the set of damper quantities based upon the sensitivity analysis. Numerical examples are conducted to demonstrate the effectiveness and validity of the proposed design method.

Keywords: optimal damper placement; multiple dampers; variable adaptive step length; nonlinear damper; simultaneous optimization

1. Introduction

Various passive dampers are being used for building structures under earthquake ground motions (Soong and Dargush 1997, Hanson and Soong 2001, Christopoulos and Filiatrault 2006, de Silva 2007, Takewaki 2009). Hysteretic steel dampers (shear deformation type, buckling restrained type), viscous wall-type dampers, viscous oil dampers, visco-elastic dampers, friction dampers are representative ones. Recently viscous oil dampers (called oil dampers hereafter) are often used from the viewpoints of stable mechanical properties, low frequency and temperature dependencies and cost effectiveness, etc. together with low cost hysteretic steel dampers. Hysteretic steel dampers are preferred in the retrofit of buildings because the strength-type performance check can be applied easily to the hysteretic dampers. It should be emphasized that, during the 2011 Tohoku (Japan) earthquake, the Osaka WTC building of 256 (m) high was shaken so hard irrespective of its long distance (800 km) from the epicenter (Takewaki *et al.* 2011). It is said that this results from the resonance of the building with the so-called long-period ground

---

*Corresponding author, Professor, E-mail:takewaki@archi.kyoto-u.ac.jp

motion. To respond to this unfavorable situation, the retrofit of this building is under planning with oil dampers and hysteretic steel dampers. Since oil dampers induce large internal forces into building frames under intensive ground motions, it is usual to introduce the so-called relief mechanism in those oil dampers. When the internal force in the oil damper arrives at the relief force, the damping coefficient becomes smaller compared to the initial one and the maximum force in the oil damper is kept in a reasonable range. In addition, inertial mass dampers are also being used as an effective damper which provides a negative stiffness and leads to the input reduction (Takewaki et al. 2012).

Many research works have been accumulated so far on the damper optimization (Zhang and Soong 1992, Tsuji and Nakamura 1996, Takewaki 1997, 2000, Takewaki and Yoshitomi 1998, Garcia 2001, Singh and Moreschi 2001, Uetani et al. 2003, Trombetti and Silvestri 2004, Liu et al. 2005, Lavan and Levy 2006, Silvestri and Trombetti 2007, Aydin et al. 2007, Cimellaro 2007, Attard 2007, Lavan and Dargush 2009, Hwang et al. 2013). While most of them deal with linear responses, quite a few treat non-linear responses in building structures or dampers (Uetani et al. 2003, Attard 2007, Lavan and Levy 2005, 2010, Cimellaro and Lavan et al. 2009, Cimellaro and Soong et al. 2009b, Whittle et al. 2012, Adachi et al. 2013). However, there is no research on the optimization of location and quantity of dampers which deals with non-linear responses and includes simple and systematic algorithms. In addition, an analytical procedure for redesign of linear buildings has been proposed which optimizes simultaneously both the structure and the structural control system in order to reduce the structural mass (Cimellaro and Soong et al., 2009a).

The purpose of this paper is to propose a practical method for simultaneous optimal use of various passive dampers (oil, hysteretic and inertial mass dampers) so as to minimize the maximum interstory drift of a shear building model subjected to a set of design earthquake ground motions under the constraint on the total cost. It is often the case in the practical building structural design that multiple dampers are used in a building. The advantages of simultaneous use of multiple dampers are to enable a fail-safe system and to construct a passive damper system with different phase properties. The response sensitivity of buildings including hysteretic dampers is high and a devised algorithm of adaptive step-length is useful to obtain a smooth and reliable response sensitivity. The proposed procedure enables structural designers to derive a series of optimal distribution of damper quantities with respect to the level of the total cost of dampers which is useful in seeking for the relation between the optimal response level and the quantity and placement of passive dampers. Numerical examples reveal some features of the optimal distribution of various passive dampers.

2. Simultaneous optimal damper placement problem using three types of dampers

2.1 Modeling of oil dampers

Consider oil dampers with a relief mechanism and a shear building model with those oil dampers. The damping force - velocity relation of an oil damper is shown in Fig. 1. The properties of oil dampers are treated as the total amount in each story.

Let c_{1j}, c_{2j}, R_j denote the initial damping coefficient of the oil damper below the relief force, the second damping coefficient of the oil damper above the relief force and the relief force in the jth story, respectively. The ratio of these initial and second damping coefficients is specified
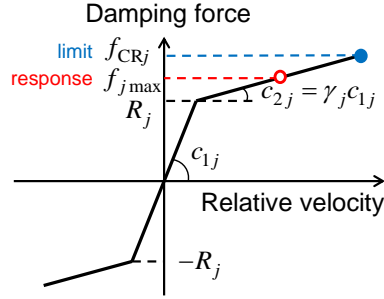
Fig. 1 Damping force-relative velocity relation of oil damper

here as $\gamma_j = c_{2j}/c_{1j} = 0.05$. The limit value of the damping force of oil dampers in the jth story is denoted by $f_{\mathrm{CR}j}$ and the ratio $f_{\mathrm{CR}j}/R_j$ is given by $f_{\mathrm{CR}j}/R_j = 1.1$. As usual, $f_{\mathrm{CR}j}$ is treated to depend on R_j

Since the shear building model including oil dampers with the relief mechanism exhibits a non-linear behavior, time-history response analysis may be inevitable for accurate response evaluation. For this reason, time-history response analysis is used here for the evaluation of responses and their sensitivities to the variation of relief forces.

Let $\delta_{j\max}$ denote the maximum interstory drift in the jth story to an earthquake ground motion. $D_{\max}$ represents the maximum value among $\{\delta_{j\max}\}$. It is useful to define the ratio $r_{j\max}$ of the maximum response damping force $f_{j\max}$ in the oil dampers in the jth story to the corresponding relief force R_j as

$$r_{j\max} = \frac{f_{j\max}}{R_j} \tag{1}$$

This quantity is called the maximum damping force ratio later.

It is usual in the ordinary earthquake resistant design of buildings to define a set of design earthquake ground motions. For this purpose, let us introduce 'envelopes' of $\delta_{j\max}$, $D_{\max}$, $r_{j\max}$ for all the design earthquake ground motions and denote them as $\hat{\delta}_{j\max}$, $\hat{D}_{\max}$, $\hat{r}_{j\max}$.

2.2 Modeling of hysteretic dampers

Steel hysteretic dampers are used in this paper. The initial stiffness $k_{\mathrm{d}j}$ and the yield displacement u_y are the major parameters to characterize the present steel hysteretic dampers. An elastic-perfectly plastic restoring force characteristic as shown in Fig. 2 is assumed.

2.3 Modeling of inertial mass dampers

Inertial mass dampers are effective for relative acceleration between two points (for example see Takewaki et al. 2012). The performance of an inertial mass damper can be characterized by the coefficient z which has the same unit as mass and denotes the coefficient of the inertial mass damper between the internal force in the inertial mass damper and the corresponding relative acceleration.

Consider a single-degree-of-freedom model with an inertial mass damper as shown in Fig. 3(a).
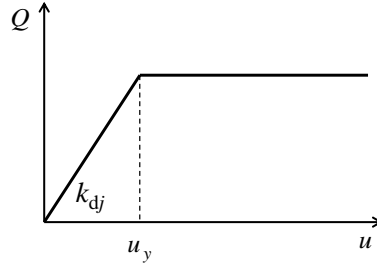
Fig. 2 Force-deformation relation of hysteretic damper

Let I_θ, θ, x and R denote the moment of inertia of the inertial mass damper, the rotation angle of the inertial mass damper, the horizontal displacement of the model and the radius of the inertial mass damper. The internal force in the inertial mass damper can then be described in terms of relative acceleration as

$$p = (I_\theta \ddot{\theta}/R) = (I_\theta/R^2)\ddot{x} = z\ddot{x} \tag{2}$$

Fig. 3(b) shows the schematic diagram of an example inertial mass damper.

Fig. 4 presents the force-deformation relations of a viscous damper, a viscoelastic damper, a hysteretic damper and an inertial mass damper. It can be understood, while the viscous damper has zero stiffness and the viscoelastic damper has positive stiffness (the hysteretic damper has dual stiffness), the inertial mass damper has a pseudo-negative stiffness.
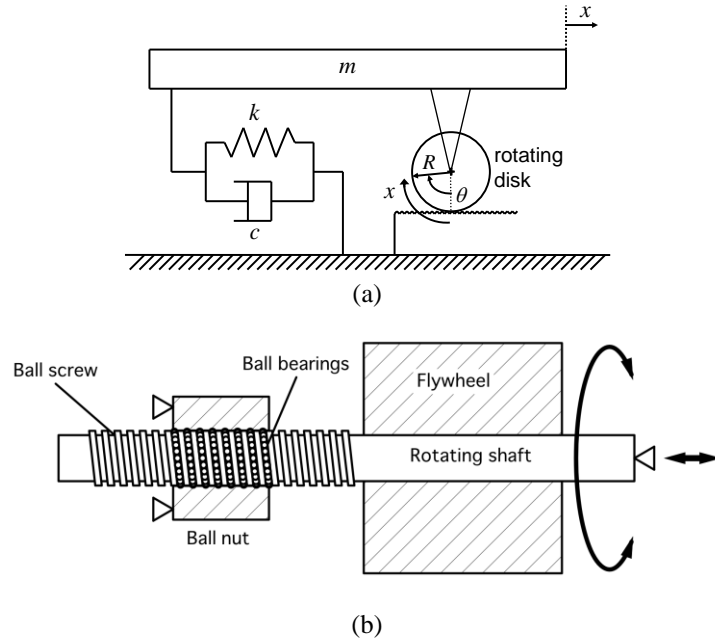

(a)

(b)

Fig.3 (a) Single-degree-of-freedom model with inertial mass damper, (b) Schematic diagram of example inertial mass damper (Takewaki et al.2012)
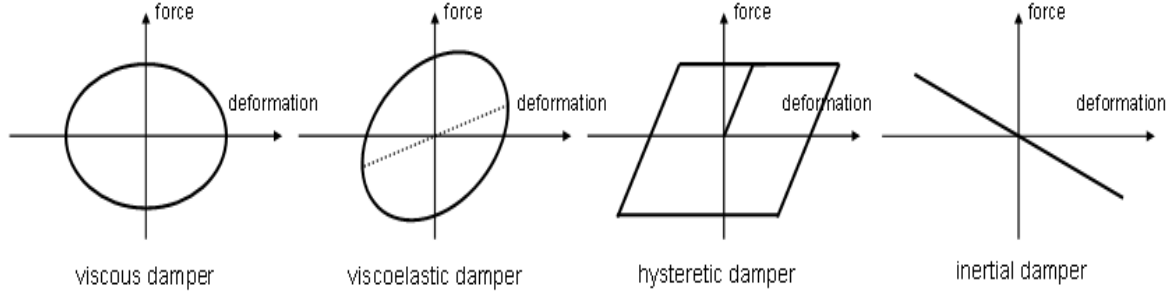
Fig. 4 Force-deformation relations of viscous damper, viscoelastic damper, hysteretic damper and inertial mass damper

Since the acceleration and the displacement have an opposite phase, the inertial mass damper has a negative stiffness. Let z_j denote the coefficient of the inertial mass damper between the internal force in the inertial mass damper.

2.4 Simultaneous optimal damper placement problem

Consider an *N*-story shear building model with oil, hysteretic and inertial mass dampers (see Figs. 5 and 6). The story stiffness of the shear building model is denoted by $\{k_{Sj}\}$. A stiffness proportional viscous damping is employed here in the main frame.

A simultaneous optimal damper placement problem can be stated as follows.

[Problem] Find the relief forces $\mathbf{R} = \{R_j\}$ of oil dampers, the initial stiffnesses $\mathbf{k}_d = \{k_{dj}\}$ of hysteretic dampers and the inertial masses $\mathbf{z} = \{z_j\}$ of inertial mass dampers so as to minimize F subject to

$$\sum_{j=1}^{N} \{Y_C R_j + Y_K k_{dj} + Y_Z z_j\} = \overline{C}_d \tag{3}$$

Y_C, Y_K and Y_Z are cost coefficients for oil, hysteretic and inertial mass dampers, respectively, which transform the mechanical properties, $\mathbf{R} = \{R_j\}$, $\mathbf{k}_d = \{k_{dj}\}$ and $\mathbf{z} = \{z_j\}$, into the cost. Actual values of these coefficients will be provided later in numerical examples.

3. Optimal damper placement problem for single type damper

3.1 Optimal placement of oil damper

Consider an *N*-story shear building model.   The design problem of oil dampers may be stated as follows.

[Problem] Find $\mathbf{R} = \{R_j\}$ so as to minimize F subject to

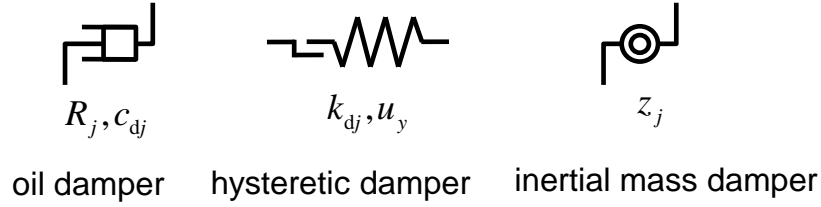$$\sum_{j=1}^{N} R_j = \overline{C}_d \tag{4}$$

$$R_j, c_{\mathrm{d}j} \qquad k_{\mathrm{d}j}, u_y \qquad z_j$$

oil damper   hysteretic damper   inertial mass damper

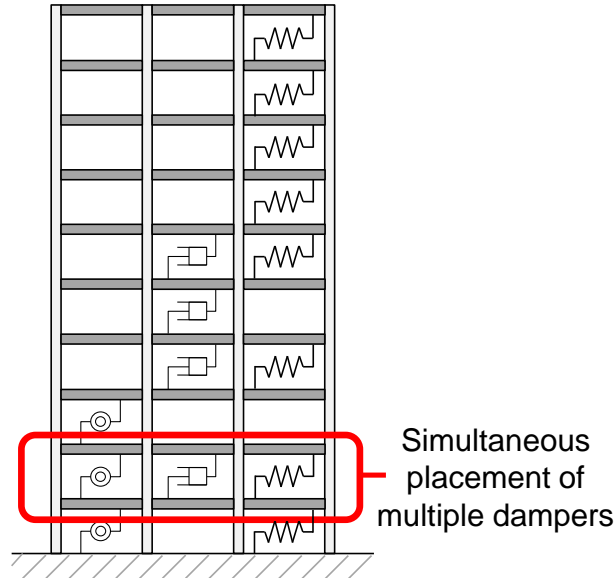Fig. 5 Oil, hysteretic and inertial mass dampers

Simultaneous placement of multiple dampers

Fig. 6 Building frame with oil, hysteretic and inertial mass dampers

$$\hat{r}_{j\max} \le \alpha \quad \left(j = 1, 2, \cdots, N \right) \tag{5}$$

In this problem, $\bar{C}_{\mathrm{d}}$ is the specified sum of relief forces and α is the common specified value of $f_{\mathrm{CR}j}/R_j$. $\hat{D}_{\max}$ is employed as F. For simplicity of expression, $\hat{D}_{\max}$ and $\hat{r}_{j\max}$ are expressed simply as $D_{\max}$ and $r_{j\max}$ later.

A practical procedure for optimal oil damper design has been proposed for reducing the computational load (Adachi et al. 2013). There are three practical aspects: (1) use of the reduced model for computational efficiency (Guyan 1965), (2) approximate algorithm to remove oil dampers in case of the violation of constraints on damping force, (3) search of a series of optimal oil damper distribution for different damper quantities.   Since a shear building model is used here, the reduced model (static condensation (Guyan 1965)) is not used. Fig.7 illustrates the approximate solution procedure. The design algorithm may be summarized as follows:

[Step 1] Adopt the response damper forces for a linear damper model as the initial relief forces of oil dampers. The sum of relief forces of oil dampers is determined here and reduced in the subsequent step.

[Step 2] Produce *N* candidates in which ΔR is reduced from the present relief force in each story.

[Step 3] Compute the maximum damping force ratio and the objective function for each model constructed in Step 2 through nonlinear time-history response analysis. If the constraint on the maximum damping force ratio is violated in one story, remove the oil damper in that story. Repeat this procedure until the constraints on the maximum damping force ratio are satisfied in all stories.

[Step 4] Select the best candidate with the minimum objective function from the candidates produced in Step 3.

[Step 5] When an oil damper is removed from the model in Step 3, the corresponding oil damper is removed. Then go to Step 2.

The most advantageous feature of the method used in this paper is to be able to obtain easily a feasible initial design satisfying the constraints on the response of nonlinear oil dampers. This can be achieved by using the maximum damping force for a 'linear' oil damper as the initial relief force of the oil damper. The damping force just attains at the relief force and does not violate the constraint on the maximum damping force (limit damping force is the relief force multiplied by the coefficient 1.1).

In the reference (Adachi *et al*. 2013), the damping coefficients of oil dampers have been adopted as fixed values. However, it has been made clear (Noshi *et al*. 2013) that the employment of the damping coefficients of oil dampers as design variables is appropriate to obtain more rational optimal placement of oil dampers. Therefore this technique (employment of the damping coefficients of oil dampers as design variables) is used also in this paper.

3.2 Optimal placement of hysteretic damper (variable adaptive step length)

Since hysteretic dampers have nonlinear stiffness properties (force has the same phase as displacement) and input earthquake ground motions are random, the seismic response of a building
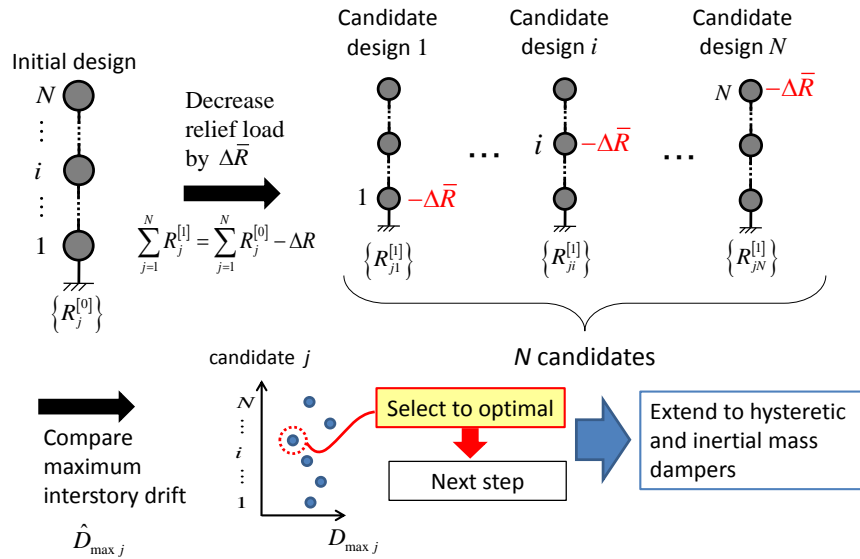

Fig. 7 Flowchart of oil damper optimization (flowchart is valid for every type of damper)

with hysteretic dampers deviates greatly depending on the installed quantity of dampers. The main issue related to displacement activated devices like hysteretic dampers is that the internal forces generated by the dampers were in phase with the maximum deformation of the structure, and as a result, the maximum forces and deformations appeared at the same time in the structure. This characteristic leads to an unfavorable effect on main structures and disturbs a reliable formulation of optimal damper placement. In order to overcome such difficulty, a new optimization method including a variable adaptive step length is proposed. Although a constraint on accumulated plastic deformation ratio is sometimes required in hysteretic dampers for long-duration earthquake ground motions, this is not taken into account here because of a simple, essential presentation of a new optimization procedure.

Fig. 8 shows a schematic diagram of the proposed sensitivity evaluation algorithm including variable adaptive step length. While a conventional finite difference algorithm focuses on the point $\overline{C}_d^{[k]} - \Delta\overline{C}_d$, several candidates $\overline{C}_d^{[k]} - \Delta\overline{C}_d$, ..., $\overline{C}_d^{[k]} - 5\Delta\overline{C}_d$ are taken into account. Here $\overline{C}_d^{[k]}$ is the current value (cost) of total damper quantity and $\Delta\overline{C}_d$ is the increment of the total damper quantity. Among these several candidates of decreased hysteretic damper cost, the decreased hysteretic damper cost attaining the lowest value of the maximum interstory drift is employed as the next-step sensitivity. Although the minimum value is used in this example, the average value or the maximum value of the maximum interstory drift can be employed in consideration of the safety level of the passively controlled buildings.

3.3 Optimal placement of inertial mass damper

Because the building with inertial mass dampers exhibits a linear response, a straightforward optimization method based on response sensitivity can be used. The response sensitivity with respect to inertial mass dampers can be computed by a finite difference scheme.
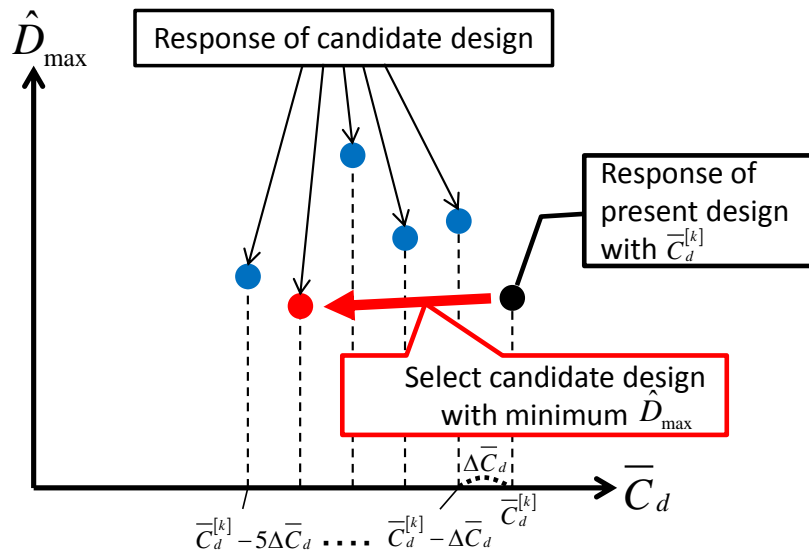

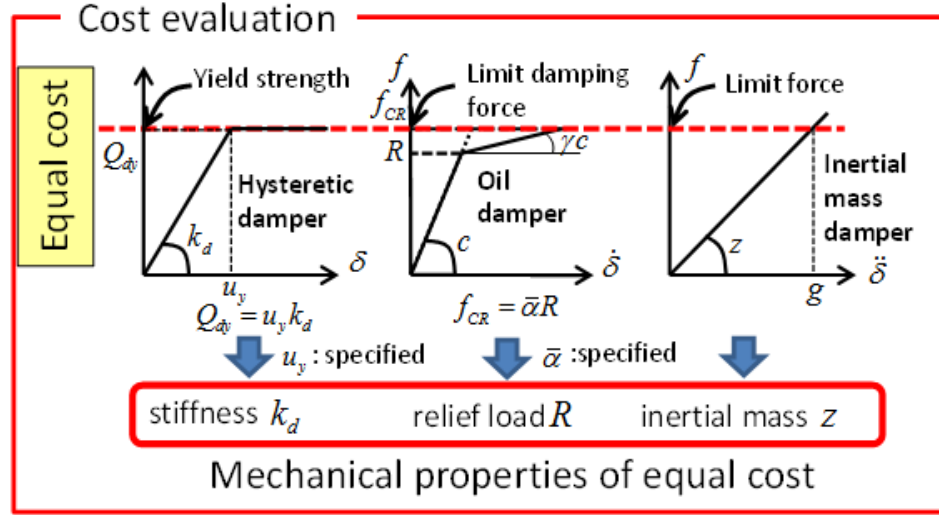Fig. 8 Sensitivity evaluation algorithm including variable adaptive step length

Fig. 9 Mechanical properties of equal cost

4. Method for simultaneous optimal damper placement using three types of dampers

4.1 Cost ratio among different dampers

The optimization procedure for each damper explained in Section 3 can be incorporated into the simultaneous optimization procedure. It is necessary to consider the cost ratios among different dampers. In other words, the quantities of mechanical properties, $\mathbf{R} = \{R_j\}$, $\mathbf{k}_d = \{k_{dj}\}$ and $\mathbf{z} = \{z_j\}$, with an equal cost should be computed at first. Those quantities for oil, hysteretic and inertial mass dampers are proportional to $1/Y_C$, $1/Y_K$ and $1/Y_Z$, respectively (see Fig. 9).

4.2 Procedure of simultaneous optimal damper placement

Fig. 10 shows the envelope response of the maximum interstory drift for multiple candidate ground motions (see Adachi et al. 2013). Although an example for two ground motions is presented here, this is applicable to a more general case for multiple ground motions. It is noted that this method does not depend largely on the number of earthquake ground motions used. It is not intended here to clarify the response characteristics to earthquake ground motions. In order to reflect the characteristics of input ground motions in the design procedure, more detailed input ground motions should be used (for example see Cimellaro 2012).

Fig. 11 presents the flowchart of simultaneous optimal damper placement. Since it is convenient to start from a design with a certain amount of dampers in case of oil dampers because of its simplicity of satisfying the response constraints on oil dampers, an initial design of a certain amount of oil, hysteretic and inertial mass dampers is also appropriate in developing a practical and systematic design procedure. It should be remarked again that the advantages of simultaneous use of multiple dampers are to enable a fail-safe system and to construct a passive damper system with different phase properties. Therefore the design with multiple dampers is not necessarily superior to the design with one type of dampers.
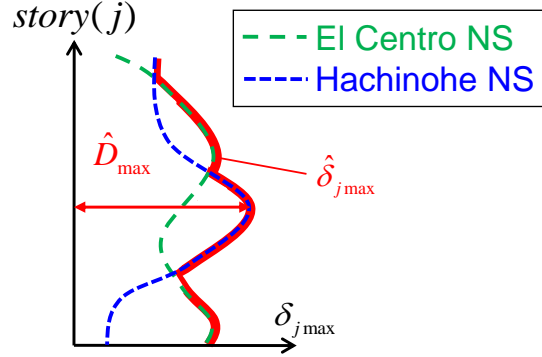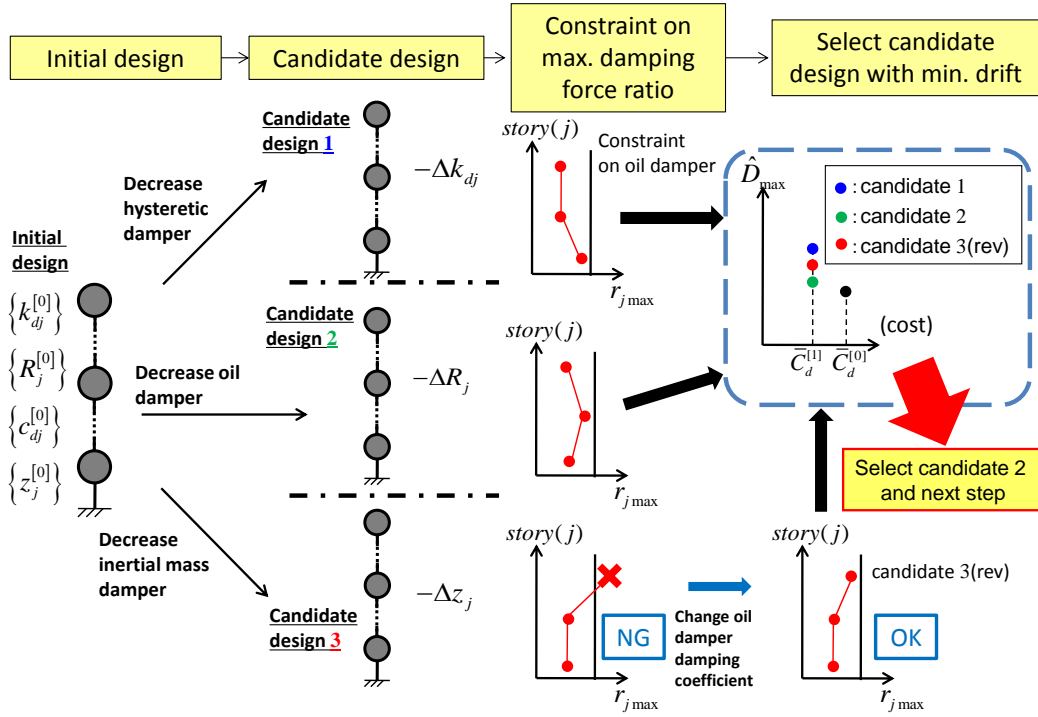
Fig. 10 Envelope response

Fig. 11 Flowchart of simultaneous optimal damper placement

4.3 Numerical examples

Two representative recorded ground motions, i.e. El Centro NS 1940 (PGV = 0.50 m/s, PGA = 5.10 m/s^2) and Hachinohe NS 1968 (PGV = 0.50 m/s, PGA = 3.33 m/s^2), are employed as the design earthquake ground motions. The envelope response as shown in Fig. 10 is used in this paper.

The 10-story main structure has been modeled into a 10-story shear building model and designed so that it has a fundamental natural period of 1.05 (s) and a realistic stiffness distribution (see Appendix 1). The constant floor mass is 1.0×10^6 kg which corresponds approximately to 30

m $\times$ 30 m floor plan. The structural damping ratio (stiffness-proportional viscous damping) is 0.02.

As explained before, the quantities of mechanical properties of equal cost for oil, hysteretic and inertial mass dampers are proportional to $1/Y_C$, $1/Y_K$ and $1/Y_Z$, respectively. These values were provided from two major building design and construction companies in Japan. The equal-cost damper quantities used as the amount of decrease in the response sensitivity computation are the relief force = 300 kN for oil dampers, the damper stiffness = 130,000 kN/m for hysteretic dampers and the inertial mass = 25,000 kg for inertial mass dampers.

Four sets of combination of the initial damper quantities have been employed in order to investigate the effect of the initial damper quantities on the effective damper quantities in the intermediate optimization process.

The initial damping coefficients of oil damper were specified constant throughout the stories so as to attain the damping ratio 0.2. As stated before, the ratio of the second-slope damping coefficient to the initial-slope coefficient is 0.05 and the ratio of the limit damping force to the relief force is 1.1. The relief forces of oil dampers in the initial design stage were prescribed as the maximum forces of linear oil dampers under the design earthquake ground motions stated above. The initial stiffness of hysteretic dampers in the initial design stage was given by specifying the cost ratio with the oil dampers and the yield displacement is 0.005 m. The inertial mass of inertial mass dampers in the initial design stage was given as well by specifying the cost ratio with the oil dampers.
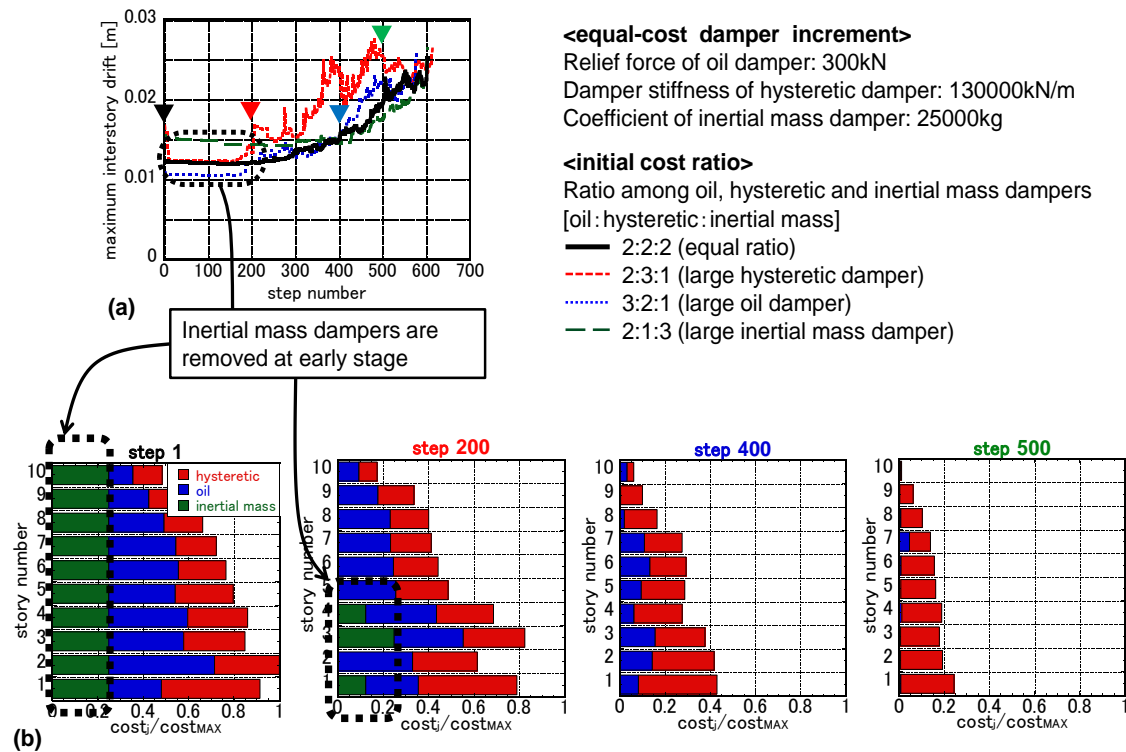

Fig. 12 (a) Maximum interstory drift with respect to step number, (b) Remaining effective damper ratio at step 1, 200, 400, 500 (Initial damper cost ratios, 2: 2: 2)
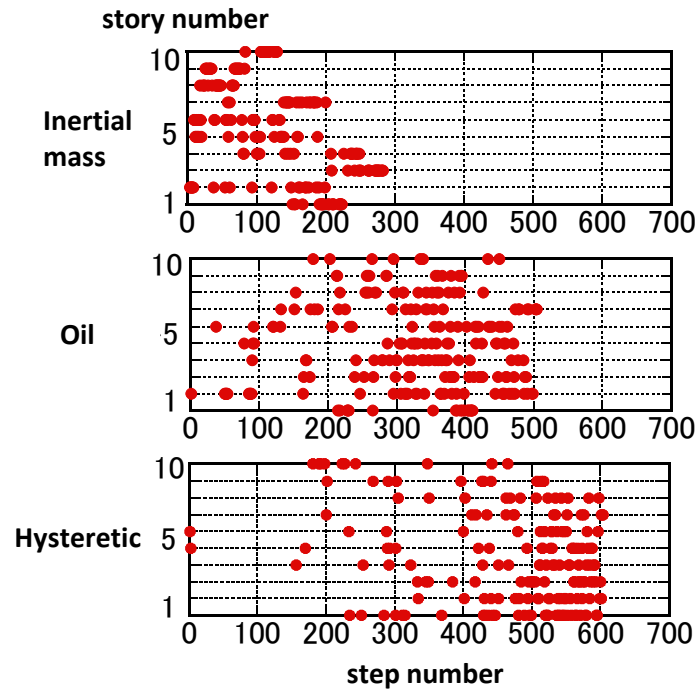
Fig.13 Step number at which each damper decreases (damper with mark at early step indicates that such damper is decreased early)

Fig. 12(a) shows the maximum interstory drift with respect to the step number in case of the initial damper cost ratios 2: 2: 2, 2: 3: 1, 3: 2: 1, 2: 1: 3 of oil, hysteretic and inertial mass dampers. It can be understood that the maximum interstory drift does not change so much until 200 steps irrespective of the initial damper cost ratios and exhibits different distributions after 200 steps depending on the initial damper quantities. When the ratio of hysteretic dampers is large in the initial step, the maximum interstory drift exhibits a non-smooth curve. This phenomenon was observed before in the case of hysteretic dampers only. The maximum ductility factors of hysteretic dampers are around 2 in the initial step and about 4-5 in later steps. Fig. 12(b) illustrates the effective damper quantities (cost ratios) at several steps. It can be observed that the inertial mass dampers are removed quickly and the hysteretic dampers remain at later steps in case of the initial damper cost ratios 2: 2: 2 of oil, hysteretic and inertial mass dampers.

Fig. 13 presents which story dampers are changed during the optimization process in case of the initial damper cost ratios 2: 2: 2 of oil, hysteretic and inertial mass dampers. The number of dots indicates the number of change (decrease of damper quantity) and the place of dots presents the time of such change.

Fig. 14 shows the effective damper quantities (cost ratios) at several steps in case of the initial damper cost ratios 2: 3: 1, 3: 2: 1, 2: 1: 3 of oil, hysteretic and inertial mass dampers. It can be observed from Fig. 11(c) and Fig. 12 that the optimal damper placement strongly depends on the initial damper cost ratios. In general, hysteretic dampers are effective in all the cases treated here and oil dampers are the next. When a large amount of inertial mass dampers are provided in the initial stage (i.e. have a large initial cost ratio to other dampers), they may remain to some steps.
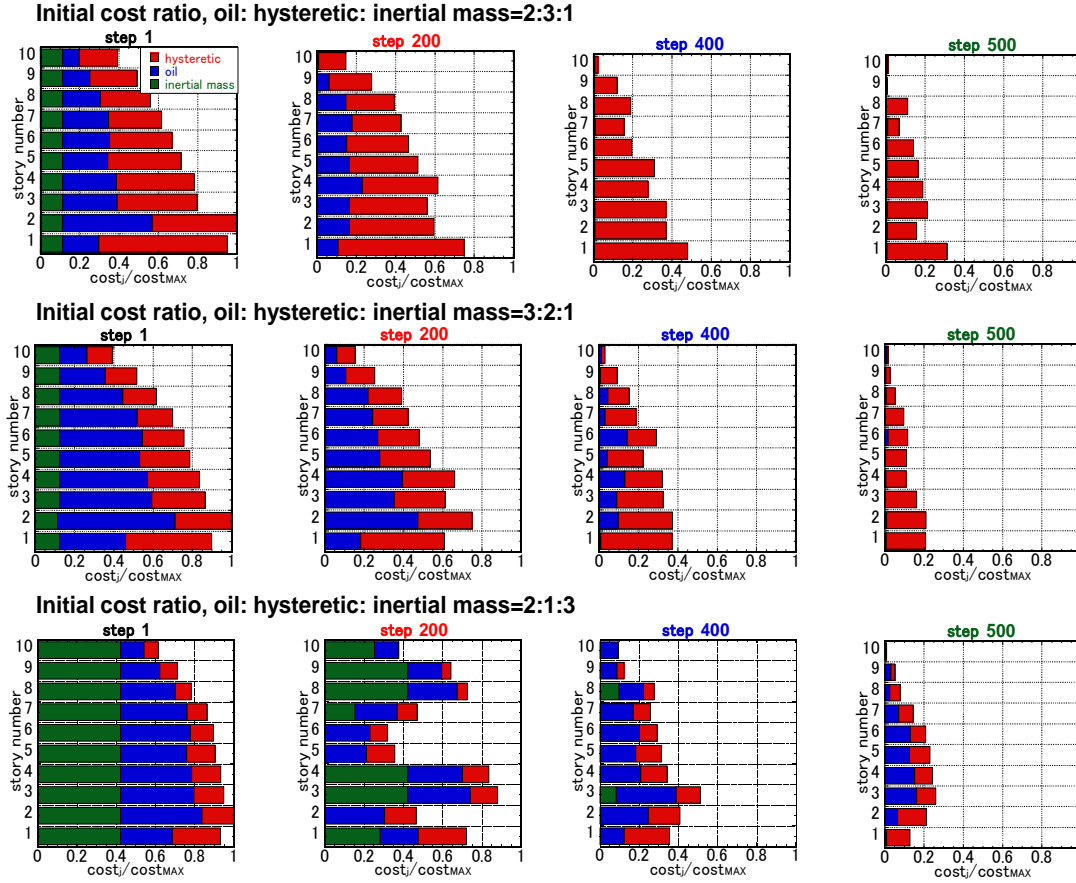
Fig. 14 Effective damper quantities and their ratios at step 1, 200, 400, 500 (Initial damper cost ratios, 2: 3: 1, 3: 2: 1, 2: 1: 3)

There is no other method because the present problem deals with nonlinear oil dampers (Adachi et al. 2013) and hysteretic dampers. The most advantageous feature is to be able to obtain easily a feasible initial design satisfying the constraints on the response of nonlinear oil dampers. With other methods, much computational work would be necessary to obtain such feasible initial design. The optimization methods for nonlinear dampers are quite difficult to develop. The present paper discussed a possibility to overcome this difficulty.

5. Conclusions

The following conclusions have been derived.
(1) The proposed method for simultaneous optimal placement of various passive dampers possesses a sensitivity analysis engine including nonlinear response analysis in the optimization process. The method enables structural designers to find an optimal passive damper in each design step. The method is general and applicable to arbitrary number of types of passive dampers.

(2) The advantages of simultaneous use of multiple dampers are to enable a fail-safe system and to construct a passive damper system with different phase properties.
(3) The response sensitivity of buildings including hysteretic dampers is high and a devised algorithm of adaptive step-length is useful to obtain a smooth and reliable response sensitivity.
(4) Since it is convenient to start from a design with a certain amount of dampers in case of oil dampers because of its simplicity of satisfying the response constraints on oil dampers, an initial design of a certain amount of oil, hysteretic and inertial mass dampers is also appropriate in developing a practical and systematic design procedure.
(5) An initial quantity of three-type passive dampers affects greatly the optimal placement of dampers.

Acknowledgements

References

Adachi, F., Yoshitomi, S., Tsuji, M. and Takewaki, I. (2013), "Nonlinear optimal oil damper design in seismically controlled multi-story building frame", *Soil Dyn. Earthq. Eng.*, **44**(1), 1-13.
Attard, T.L. (2007), "Controlling all interstory displacements in highly nonlinear steel buildings using optimal viscous damping", *J. Struct. Eng. –* ASCE, **133**(9), 1331-1340.
Aydin, E., Boduroglub, M.H. and Guney, D. (2007), "Optimal damper distribution for seismic rehabilitation of planar building structures", *Eng. Struct.*, **29**, 176-185.
Cimellaro, G.P. (2007), "Simultaneous stiffness-damping optimization of structures with respect to acceleration, displacement and base shear", *Eng. Struct.*, **29**, 2853-2870.
Cimellaro, G.P. (2012), "Correlation in spectral accelerations for earthquakes in Europe" *Earthq. Eng. Struct. Dyn.*, Article first published online: 7 SEP 2012 DOI: 10.1002/eqe.2248.
Cimellaro, G.P., Lavan, O. and Reinhorn, A.M. (2009), "Design of passive systems for controlled inelastic structures", *Earthq. Eng. Struct. Dyn.*, **38**(6), 783-804.
Cimellaro, G.P., Reinhorn, A.M. and De_Stefano, A. (2011), "Introspection on improper seismic retrofit of Basilica Santa Maria di Collemaggio after 2009 Italian earthquake", *Earthq. Eng. Eng. Vib.*, **10**(1), 153-161.
Cimellaro, G.P., Soong, T.T. and Reinhorn, A.M. (2009a), "Integrated design of controlled linear structural systems", *J. Struct. Eng. – ASCE*, **135**(7), 853-862.
Cimellaro, G.P., Soong, T.T. and Reinhorn, A.M. (2009b), "Integrated design of inelastic controlled structural systems", *Struct.Control Health Monitor.*, **16**, 689-702.
Christopoulos, C. and Filiatrault, A. (2006), *Principle of passive supplemental damping and seismic isolation*, IUSS Press, University of Pavia, Italy.
de Silva CW (ed.) (2007), *Vibration damping, control, and design*, CRC Press.
Garcia, D.L. (2001), "A simple method for the design of optimal damper configurations in MDOF structures", *Earthq. Spectra*, **17**, 387-398.
Guyan, R.J. (1965), "Reduction of stiffness and mass matrices", *AIAA J.*, **3**, 380.
Hanson, R.D. and Soong, T.T. (2001), *Seismic design with supplemental energy dissipation devices*, EERI, Oakland, CA.

Hwang, J.S., Lin, W.C. and Wu, N.J. (2013), "Comparison of distribution methods for viscous damping coefficients to buildings", *Struct. Infrastruct. Eng.*, **9**(1), 28-41.

Lavan, O. and Dargush, G.F. (2009), "Multi-objective evolutionary seismic design with passive energy dissipation systems", *J. Earthq. Eng.*, **13**(6), 758-790.

Lavan, O. and Levy, R. (2005), "Optimal design of supplemental viscous dampers for irregular shear-frames in the presence of yielding", *Earthq. Eng. Struct. Dyn.*, **34**(8), 889-907.

Lavan, O. and Levy, R. (2006), "Optimal design of supplemental viscous dampers for linear framed structures", *Earthq. Eng. Struct. Dyn.*, 35, 337-356**.**

Lavan, O. and Levy, R. (2010), "Performance based optimal seismic retrofitting of yielding plane frames using added viscous damping", *Earthq. Struct.*, **1**(3), 307-326.

Liu, W., Tong, M. and Lee, G. (2005), "Optimization methodology for damper configuration based on building performance indices", *J. Struct. Eng.- ASCE*, **131**(11), 1746-1756.

Noshi, K., Yoshitomi, S., Tsuji, M. and Takewaki, I. (2013), "Optimal nonlinear oil damper design in seismically controlled multi-story buildings for relief forces and damping coefficients", *J. Struct. Eng.*, Architectural Institute of Japan, Vol. 59B. (in Japanese)

Silvestri, S. and Trombetti, T. (2007), "Physical and numerical approaches for the optimal insertion of seismic viscous dampers in shear-type structures", *J. Earthq. Eng.*, **11**, 787-828.

Singh, M.P. and Moreschi, L.M. (2001), Optimal seismic response control with dampers, *Earthq. Eng. Struct Dyn.*, 30, 553-572.

Soong, T.T. and Dargush, G.F. (1997), *Passive energy dissipation systems in structural engineering*, John Wiley & Sons, Chichester.

Takewaki, I. (1997), "Optimal damper placement for minimum transfer functions", *Earthq. Eng. Struct. Dyn.*, **26**, 1113-1124.

Takewaki, I. (2009), *Building control with passive dampers: optimal performance-based design for earthquakes*, John Wiley & Sons Ltd. (Asia)

Takewaki, I. (2000), "Optimal damper placement for planar building frames using transfer functions", *Struct. Multidiscip. Opt.*, **20**(4), 280-287.

Takewaki, I., Murakami, S., Fujita, K., Yoshitomi, S. and Tsuji, M. (2011), "The 2011 off the Pacific coast of Tohoku earthquake and response of high-rise buildings under long-period ground motions", *Soil Dyn. Earthq. Eng.*, **31**(11), 1511-1528.

Takewaki, I., Murakami, S., Yoshitomi, S. and Tsuji, M. (2012), "Fundamental mechanism of earthquake response reduction in building structures with inertial dampers", *Struct. Control Health Monitor.*, **19**(6), 590-608.

Takewaki, I. and Yoshitomi, S. (1998), "Effects of support stiffnesses on optimal damper placement for a planar building frame", *J. Struct. Des. Tall Build.*, **7**(4), 323-336.

Trombetti, T. and Silvestri, S. (2004), "Added viscous dampers in shear-type structures: the effectiveness of mass proportional damping", *J.Earthq. Eng.*, **8**(2), 275-313.

Tsuji, M. and Nakamura, T. (1996), "Optimum viscous dampers for stiffness design of shear buildings", *J. Struct. Des. Tall Build.*, **5**, 217-234.

Tsuji, M., Tanaka, H., Yoshitomi, S. and Takewaki, I. (2011), "Model reduction method for buildings with viscous dampers under earthquake loading", *J. Struct. Construct. Eng.*, Architectural Institute of Japan, **76**(665), 1281-1290. (in Japanese)

Uetani, K., Tsuji, M. and Takewaki, I. (2003), "Application of optimum design method to practical building frames with viscous dampers and hysteretic dampers", *Eng. Struct.*, **25**, 579-592.

Whittle, J.K., Williams, M.S., Karavasilis, T.L. and Blakeborough, A. (2012), "A comparison of viscous damper placement methods for improving seismic building design", *J. Earthq. Eng.*, **16**(4), 540-560.

Zhang, R.H. and Soong, TT. (1992), "Seismic design of viscoelastic dampers for structural applications", *J. Struct. Eng.- ASCE*, **118**, 1375-1392.

CC

276   *Yu Murakami, Katsuya Noshi, Kohei Fujita, Masaaki Tsuji and Izuru Takewaki*

Appendix 1: Story stiffness of 10-story main frame

A 10-story main frame has been modeled into a 10-story shear building model. The 10-story shear building model is designed so that it possesses a fundamental natural period of 1.05(s) and a realistic stiffness distribution listed below. The constant floor mass is 1.0×10^6 kg which corresponds approximately to 30 m × 30 m floor plan. The structural damping ratio (stiffness-proportional viscous damping) is 0.02.

Story	Story stiffness [N/m]
1	15.1×10^8
2	9.96×10^8
3	9.42×10^8
4	9.19×10^8
5	8.87×10^8
6	7.31×10^8
7	6.25×10^8
8	5.92×10^8
9	5.55×10^8
10	4.50×10^8